LUNAR ORIENTALE BASIN: TOPOGRAPHIC CHARACTERIZATION FROM LUNAR ORBITING LASER ALTIMETER (LOLA) DATA AND INSIGHTS INTO MULTI-RINGED BASIN FORMATION.

J. L. Dickson[1], J. W. Head[1], D. E. Smith[2], M. T. Zuber[3], G. Neumann[2], C. Fassett[1] and the LOLA Team. [1]Brown Univ., Providence, RI (james_dickson@brown.edu), [2]NASA GSFC, Greenbelt, MD, [3]MIT, Cambridge, MA.

Introduction: The 930 km diameter Orientale basin is the youngest and most well-preserved large multi-ringed impact basin on the Moon [1-10]; it has not been significantly filled with mare basalts, as have other lunar impact basins, and thus the nature of the basin interior deposits and ring structures are very well-exposed and provide major insight into the formation and evolution of planetary multi-ringed impact basins [1-10] (Fig. 1). New data from the armada of recent and ongoing lunar spacecraft are providing multiple data sets, new characterization, and new insights into the origin and evolution of the Orientale basin [11-15].

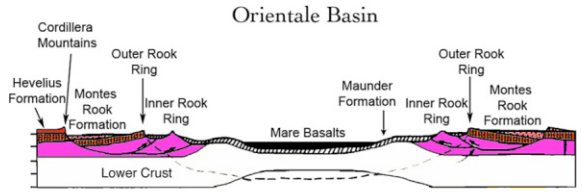

Fig. 1. Schematic cross section of the Orientale basin illustrating the relation of the basin rings to basin deposits (interior and exterior) [4].

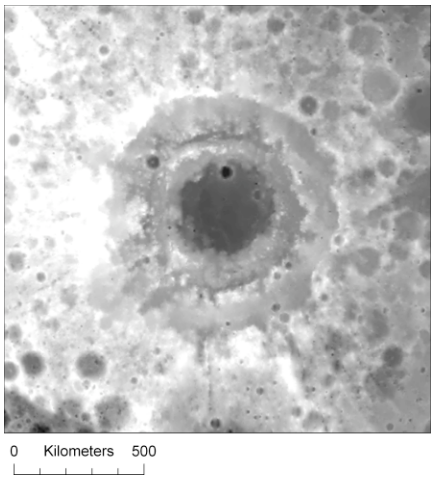

Fig. 2. LOLA altimetry map of the Orientale basin region (1/16th degree resolution).

Lunar Orbiting Laser Altimeter Data: We report here on the acquisition of new altimetry data for the Orientale basin from the Lunar Orbiting Laser Altimeter (LOLA) on board the Lunar Reconnaissance Orbiter (Fig. 1,2). We analyze the new topography, characterize the pre-basin, basin and ring topography, and outline new insights into basin formation and evolution.

Pre-basin topography: There is a broad W-E decrease in elevation, consistent with regional changes in crustal thickness [15]. Pre-basin topography had a major effect on the formation of Orientale; we have mapped dozens of impact craters underlying both the Orientale ejecta (Hevelius Formation-HF) (Fig. 2; see rough terrain between -5 and +10 degrees in Fig. 3) and the unit between the basin rim (Cordillera ring-CR) and the Outer Rook ring (OR) (known as the Montes Rook Formation-MRF) (Fig.1), ranging up in size to the Mendel-Rydberg basin just to the south of Orientale (Fig. 2;3-left); this crater-basin topography has influenced the topographic development of the basin rim (CR), sometimes causing the basin rim (see peaks in Fig. 3) to lie at a topographically lower level than the inner basin rings (OR and Inner Rook-IR). LOLA data show the pre-Orientale Grimaldi basin (Fig. 2, upper right) and several crater-basin structures in excess of 200 km. Several ghost craters are observed in LOLA data between the Cordillera and the Outer Rook ring [1], but not inside the Outer Rook. A dark ring previously thought to represent a crater partly located inside the IR [16] is now known to be a pyroclastic deposit from an eruption plume [17]. The deposits inside the OR are dominated by the Maunder Formation (MF) (Fig. 1) which consists of smooth plains (on the inner basin depression walls and floor) and corrugated deposits (on the IR plateau); this topographic configuration supports the interpretation that the MF consists of different facies of impact melt.

Basin Interior Topography: The total basin interior topography is highly variable and typically ranges ~6-7 km below the surrounding pre-basin surface, with significant variations in different quadrants (Fig. 1-4). The CR consists of linear and cuspate inward-facing scarps; continuity is interrupted by radial crater chains, and amplitude

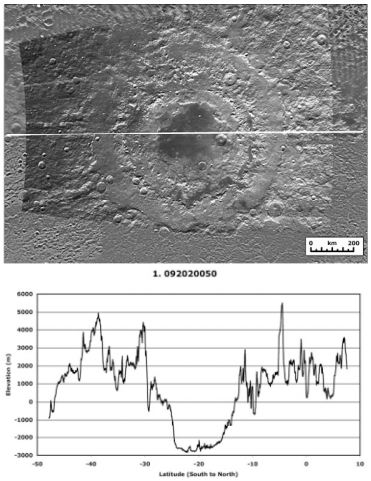

Fig. 3. LOLA profile 092020050 through the center of the Orientale basin and into the pre-Orientale Mendel-Rydberg basin to the south (left).

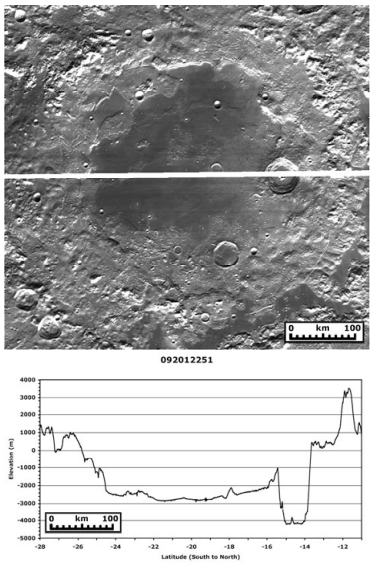

Fig. 4. LOLA profile 092012251 through the center of the Orientale basin and the 55 km diameter crater Maunder on the northern part of the inner basin floor (right).

varies due to pre-existing topography (very high in southern quadrant due to M-R basin rim; lower in east quad due to intersecting pre-existing basin and crater interiors). Between the OR and CR, topography dips away from the OR to the base of the CR; lowest depressions are often filled with mare. The OR is generally continuous topographically and consists of a set of asymmetrical massifs with steeper scarps facing inward, prominent near-rim crest topography, and transitioning outward to the outward sloping MRF surface. Compared to the CR, the OR is often much more sinuous in outline, with numerous re-entrants. The IR ring is characterized by a ring of peaks and massifs situated on a broad plateau between the inner depression and the OR, surrounded and sometimes covered by Maunder Formation, interpreted to be impact melt. The plateau itself is very rough (Fig. 2-4) and LOLA data reveal the presence of a narrow 10-25 km wide deep depression between the plateau and the base of the OR ring. This depression is often over a km deep, and is floored by impact melt and mare deposits.

The topography of the western quadrant is highly variable compared to the rest of the basin interior; here the CR and OR rings are much less distinctive, the topography between the CR and MR is higher and radial structure is more prominent, and the IR is subdued except for a very prominent arrow-shaped massif at ~225° (Fig. 2). This asymmetry is paralleled in the HF in that secondary crater chains are much more prominent in the western than eastern quadrant.

Nature of the inner basin depression: The inner basin depression is about 2-4 km deep below the IR plateau (Fig. 2,4); although some of this topography is due to post-basin-formation thermal response to impact energy input and uplifted isotherms [5], a significant part of it may be related to the initial short-term collapse of an inner melt cavity, as outlined in the nested melt cavity model of ringed basin formation [18-19]. The inner depression is floored by tilted mare basalt deposits surrounding a central pre-mare high of several hundred meters elevation and deformed by wrinkle ridges with similar topographic heights (Fig. 4); these data permit the assessment of basin loading and flexure by mare basalts and ongoing basin thermal evolution.

Location of the basin rim and excavation cavity: In contrast to some previous interpretations [see summary in 16], the distribution of these features and deposits supports the interpretation that the OR ring (Fig. 1) is the closest approximation to the basin excavation cavity. The prominence of the pre-Orientale craters right up to the Cordillera ring, the outward-sloping surface of the MRF, the ghost craters between the Cordillera and Outer Rook, all support the model that the Cordillera ring represents failure of the rim crest (Outer Rook ring) at the structural uplift hinge line, and collapse inward to form a megaterrace [1,4,19].

Post-basin impact craters and sampling depths: The depth of the 55 km diameter post-Orientale Maunder crater, located at the edge of the inner depression, is in excess of 3 km (Fig. 4); this depth permits the quantitative assessment of the nature of the deeper sub-Orientale material sampled by the crater. The mineralogy of the Orientale deposits favors the interpretation that the Orientale basin sampling depth was largely confined to the upper crust [13-15]; the mineralogy of the central peaks of the post-Orientale 55 km diameter Maunder crater, located in the basin interior depression inward of the IR (Fig. 4), are somewhat enriched in low-Ca pyroxene apparently sampling noritic lower crust, but not mantle [15].

Origin of basin rings in multi-ringed basins: These new data for the Orientale basin provide insight into basin ring formation, supporting a model that includes the expansion of a peak-ring basin by addition of an outer (Cordillera) ring by inward collapse at the edge of structural uplift along the base of the displaced zone, and the addition of an inner depression formed from an expanding nested melt cavity, and its collapse [18,19]. The newly documented annular depression at the base of the OR is interpreted to be formed during the inward collapse of the peak-ring bounded inner melt cavity.

References: 1. J. Head, Moon 11, 327, 1974; 2. K. Howard et al., RGSP 12, 309, 1974; 3. J. McCauley, PEPI 15, 220, 1977; 4. J. Head et al., JGR 98, 17149, 1993; 5. S. Bratt et al., JGR 90, 3049, 1985; 6. P. Spudis et al., JGR 89, C197, 1984; 7. B. Hawke et al., JGR 108, 5050, 2003; 8. B. Hawke et al., GRL 18, 2141, 1991. 9. C. Pieters et al., JGR 98, 17127, 1993; 10. B. Bussey & P. Spudis, GRL 24, 445, 1997; JGR 105, 4235, 2000; 11. T. Matsunaga et al., GRL 35, L232012008, 2008; 12. M. Ohtake et al., Nature 461, 236, 2009; 13. C. Pieters et al., LPSC 40, 2052, 2157, 2009; 14. S. Kumar et al., LPSC 40, 1584, 2009; 15. M. Wieczorek et al., Rev. Min. Geochem., 60, 221, 2006; 16. P. Spudis, Geology of Multi-Ringed Basins, 263 p., 1993; 17. J. Head et al., JGR, 107, 1413, 2002; 18. M. Cintala and R. Grieve, MAPS, 33, 889, 1998; 19. J. Head, GRL, in review, 2009.